Parameterized models for crosstalk analysis in high-speed interconnects

Francesco Ferranti, Tom Dhaene, Luc Knockaert
Department of Information Technology (INTEC)
Ghent University - IBBT,
Sint Pietersnieuwstraat 41, 9000, Ghent, Belgium
Email: francesco.ferranti@intec.ugent.be;
tom.dhaene@intec.ugent.be; luc.knockaert@intec.ugent.be

Giulio Antonini
Dipartimento di Ingegneria Elettrica e dell'Informazione
Università degli Studi dell'Aquila
I-67040 Monteluco di Roio, L'Aquila, Italy
Email: giulio.antonini@univaq.it

***Abstract*—We present a new parametric macromodeling technique for lossy and dispersive multiconductor transmission lines (MTLs), that is suitable to interconnect modeling. It is based on a recently introduced spectral approach for the analysis of lossy and dispersive MTLs extended by utilizing the Multivariate Orthonormal Vector Fitting (MOVF) technique to build parametric macromodels in a rational form. They can handle design parameters, such as substrate or geometrical layout features, in addition to frequency. The presented technique is suited to generate state-space models and synthesize equivalent circuits, which can be easily embedded into conventional SPICE-like solvers. Parametric macromodels allow to carry out design space exploration, design optimization and crosstalk analysis efficiently. A numerical example validates the proposed approach in both frequency and time domain and is focused on the crosstalk analysis.**

I. Introduction

To assist microwave designers, accurate modeling of previously neglected second order effects, such as crosstalk, reflection and delay, becomes increasingly important during circuit and system simulations, as the feature size and density of integrated circuits (ICs) decrease, while the signal speeds increase. The accurate prediction of these interconnects effects is fundamental for a successful design and requires the solution of large systems of equations which are often prohibitively CPU expensive [1]- [2]. Over the years, many MTL macromodeling techniques have been developed [3]- [16].

Recently, a spectral approach has been proposed for the analysis of lossy and dispersive MTLs [17], based on the computation of the closed-form dyadic Green's function of the 1-D wave propagation problem, that is expanded in a series form of orthonormal basis functions. The major advantage of such an approach over existing techniques consists of the rational nature of the dyadic Green's function which is well suited for poles and residues identification and, thus, for time-domain macromodeling purposes. Furthermore, the use of orthonormal basis functions to expand the dyadic Green's function allows to compute the poles and residues of the system independently for each mode, so reducing the complexity of the system identification significantly.

Parametric macromodels are important for design space exploration, design optimization and crosstalk analysis. In dense circuits with high operative signal bandwidths, electromagnetic coupling (crosstalk) between closely spaced signal lines limits interconnect performance [18] and becomes an important aspect of circuit design [19]. Parametric macromodeling techniques that take into account design parameters in addition to frequency (or time) are needed to perform these design activities efficiently, as their realization by full electromagnetic simulations on the entire parameter space is often computationally expensive. Some techniques for parametric macromodeling of MTLs were proposed in the framework of model order reduction [20]- [21]. Recently, a parametrization scheme based on the generalized method of characteristics (MoC) was presented [22]. We developed a new parametric macromodeling technique, presented in this paper, based on the spectral approach presented in [17] for lossy and dispersive MTLs, coupled with the Multivariate Orthonormal Vector Fitting (MOVF) technique [23] to handle other design parameters in addition to frequency. The MOVF technique builds rational parametric macromodels starting from multivariate data samples in the parameter space and combines the use of an iterative least squares estimator and orthonormal rational functions, based on a prescribed set of poles. The multivariate model can easily be reduced to a univariate frequency-dependent model in a rational form, once a set of design parameters values is fixed. The rational model is suitable to generate a finite state-space representation and an equivalent SPICE circuit by using standard realization [24] and circuit synthesis techniques [25].

The organization of this paper is as follows. First, an overview of the spectral approach for MTLs is given in Section II. Then, Section III explains how MOVF and the previous method are coupled to build a parametric representation of a MTL system. Finally, a numerical example focused on the crosstalk analysis is presented in Section IV, validating the proposed technique.

II. Modal decomposition

The general solution for the voltage at abscissa z of the multiconductor transmission line due to the port currents can be obtained through the impedance matrix $\boldsymbol{Z}$ representation [3].

978-1-4244-4267-6/09/$25.00 ©2009 IEEE

An alternative approach based on the dyadic Green's function for the 1-D wave propagation problem is presented in [17]. According to this methodology, the voltage at abscissa z, at complex frequency s, can be computed as

$$\begin{aligned} \boldsymbol{V}(z,s) &= \int_0^{\ell} \underline{\boldsymbol{G}}_V(z,z',s)\left(-\boldsymbol{Z}_{pul}(s)\boldsymbol{I}_S(z',s)\right)dz' \quad (1)\\ &= \underline{\boldsymbol{G}}_V(z,0,s)\left(-\boldsymbol{Z}_{pul}(s)\boldsymbol{I}(0,s)\right)\\ &+ \underline{\boldsymbol{G}}_V(z,\ell,s)\left(-\boldsymbol{Z}_{pul}(s)\boldsymbol{I}(\ell,s)\right). \end{aligned}$$

where the dyadic Green's function $\underline{\boldsymbol{G}}_V(z,z',s)$ for the multiconductor transmission line problem is:

$$\underline{\boldsymbol{G}}_V(z,z',s) = -\sum_{n=0}^{\infty}\phi_n(s)A_n^2\psi_n(z)\psi_n(z'), \quad (2)$$

and

$$\begin{aligned} \boldsymbol{\gamma}^2(s) &= \boldsymbol{Z}_{pul}(s)\boldsymbol{Y}_{pul}(s), & (3a)\\ \phi_n(s) &= \left[\boldsymbol{\gamma}^2(s)+\left(\frac{n\pi}{\ell}\right)^2\boldsymbol{U}\right]^{-1}, & (3b)\\ \psi_n(z) &= \cos\left(\frac{n\pi}{\ell}z\right), & (3c)\\ \psi_n(z') &= \cos\left(\frac{n\pi}{\ell}z'\right), & (3d) \end{aligned}$$

and $A_0=\sqrt{1/\ell}, A_n=\sqrt{2/\ell},\ n=1,\cdots,\infty$, $\boldsymbol{U}$ is the unitary dyadic. Finally, the spectral representation of the $\boldsymbol{Z}$ matrix is generated as:

$$\begin{aligned} \begin{bmatrix} \boldsymbol{V}(0,s)\\ \boldsymbol{V}(\ell,s)\end{bmatrix} &= \begin{bmatrix} \boldsymbol{Z}_{11} & \boldsymbol{Z}_{12}\\ \boldsymbol{Z}_{21} & \boldsymbol{Z}_{22}\end{bmatrix}\cdot\begin{bmatrix}\boldsymbol{I}(0,s)\\ \boldsymbol{I}(\ell,s)\end{bmatrix}\\ &= \sum_{n=0}^{\infty}\begin{bmatrix} \boldsymbol{Z}_{n,11} & \boldsymbol{Z}_{n,12}\\ \boldsymbol{Z}_{n,21} & \boldsymbol{Z}_{n,22}\end{bmatrix}\cdot\begin{bmatrix}\boldsymbol{I}(0,s)\\ \boldsymbol{I}(\ell,s)\end{bmatrix}, \quad (4) \end{aligned}$$

where

$$\begin{aligned} \boldsymbol{Z}_{11} &= \boldsymbol{Z}_{22} & (5a)\\ &= \sum_{n=0}^{\infty}\left[\boldsymbol{\gamma}^2(s)+\left(\frac{n\pi}{\ell}\right)^2\boldsymbol{U}\right]^{-1}\cdot A_n^2\boldsymbol{Z}_{pul}(s),\\ \boldsymbol{Z}_{12} &= \boldsymbol{Z}_{21} & (5b)\\ &= \sum_{n=0}^{\infty}\left[\boldsymbol{\gamma}^2(s)+\left(\frac{n\pi}{\ell}\right)^2\boldsymbol{U}\right]^{-1}\cdot A_n^2\boldsymbol{Z}_{pul}(s)\cos(n\pi). \end{aligned}$$

It is composed of an infinite number of modes $\boldsymbol{Z}_n$. The poles of the MTL can be evaluated as the zeros of the function of the complex variable s at the denominator of the dyadic Green's function (2):

$$\boldsymbol{\mathcal{P}}_n(s) = \det\left[\boldsymbol{\gamma}^2(s)+\left(\frac{n\pi}{\ell}\right)^2\boldsymbol{U}\right] = 0. \quad (6)$$

Modeling frequency-dependent phenomena, such as skin effect, proximity effect and dielectric polarization losses, call for numerical computation of the per-unit-length parameters which are commonly evaluated at discrete frequency samples $s_k=j\omega_k, \omega_k=2\pi f_k, k=1,\cdots,K$ by means of 2-D solvers [26]. In order to build a rational model of the dyadic Green's function, the per-unit-length longitudinal impedance $\boldsymbol{Z}_{pul}(s_k)$ and transversal admittance $\boldsymbol{Y}_{pul}(s_k)$ are to be written in a rational form of the complex variable s:

$$\boldsymbol{Z}_{pul}(s) = \boldsymbol{R}_0 + \sum_{q=1}^{P_{Z_{pul}}}\frac{\boldsymbol{R}_{Z_{pul}}}{s-p_{q,Z_{pul}}}, \quad (7a)$$

$$\boldsymbol{Y}_{pul}(s) = \boldsymbol{G}_0 + \sum_{q=1}^{P_{Y_{pul}}}\frac{\boldsymbol{R}_{Y_{pul}}}{s-p_{q,Y_{pul}}}. \quad (7b)$$

The final rational model for the $\boldsymbol{Z}$ matrix is obtained as shown in [17].

III. Parametric macromodeling of per-unit-length parameters

The MOVF technique [23] is used to generate rational parametric macromodels of the per-unit-length impedance and admittance. For ease of notation, we consider only bivariate systems in this section, but of course the full multivariate formulation can be derived in a similar way. The length is not a parameter in this parametric macromodeling strategy.

$$\begin{aligned} \boldsymbol{Z}_{pul}(s,g) &\simeq \tilde{\boldsymbol{Z}}_{pul}(s,g) = \frac{\boldsymbol{N}_{Z_{pul}}(s,g)}{D_{Z_{pul}}(s,g)}\\ &= \frac{\sum_{p=0}^{P_{Z_{pul}}}\sum_{v=0}^{V_{Z_{pul}}}\boldsymbol{c}_{pv,Z_{pul}}\phi_p(s)\varphi_v(g)}{\sum_{p=0}^{P_{Z_{pul}}}\sum_{v=0}^{V_{Z_{pul}}}\tilde{c}_{pv,Z_{pul}}\phi_p(s)\varphi_v(g)} \quad (8) \end{aligned}$$

$$\begin{aligned} \boldsymbol{Y}_{pul}(s,g) &\simeq \tilde{\boldsymbol{Y}}_{pul}(s,g) = \frac{\boldsymbol{N}_{Y_{pul}}(s,g)}{D_{Y_{pul}}(s,g)}\\ &= \frac{\sum_{p=0}^{P_{Y_{pul}}}\sum_{v=0}^{V_{Y_{pul}}}\boldsymbol{c}_{pv,Y_{pul}}\phi_p(s)\varphi_v(g)}{\sum_{p=0}^{P_{Y_{pul}}}\sum_{v=0}^{V_{Y_{pul}}}\tilde{c}_{pv,Y_{pul}}\phi_p(s)\varphi_v(g)} \quad (9) \end{aligned}$$

where s is the complex frequency variable and g is a real design variable. The maximum order of the corresponding basis functions $\phi_p(s)$ and $\varphi_v(g)$ is denoted by $P_{Z_{pul}}$, $V_{Z_{pul}}$ and $P_{Y_{pul}}$, $V_{Y_{pul}}$ respectively for $\boldsymbol{Z}_{pul}(s,g)$ and $\boldsymbol{Y}_{pul}(s,g)$. The basis functions $\phi_p(s)$ and $\varphi_v(g)$ are chosen in partial fraction form and based on a prescribed set of poles. The MOVF algorithm pursues the identification of the model coefficients $\boldsymbol{c}_{pv,Z_{pul}}$, $\tilde{c}_{pv,Z_{pul}}$ and $\boldsymbol{c}_{pv,Y_{pul}}$, $\tilde{c}_{pv,Y_{pul}}$ of numerator and denominator in (8)-(9), starting from a set of data samples $\{(s,g)_k, Z_{pul}(s,g)_k\}_{k=1}^K$ and $\{(s,g)_k, Y_{pul}(s,g)_k\}_{k=1}^K$. A linear approximation to this nonlinear optimization problem is obtained by using an iterative least squares estimator. In this work the MOVF technique is applied to matrices and it is assumed that the different matrix entries share the same poles, so the same denominator. Once these per-unit-length parametric macromodels are built, given a fixed set of values for the design parameters, they can be reduced to univariate frequency-dependent functions as in [23]. The stability of the univariate models can be imposed in the reduction step using pole flipping, and, subsequently, passivity can be enforced in a post-processing step by means of standard techniques (see [27] and [28]).

After these steps, a univariate rational model is obtained for the $\boldsymbol{Z}$ matrix as shown in [17]. At this stage, the length of the MTL system is chosen. This rational model is passive and stable, if passivity and stability are imposed on the univariate models of the per-unit-length impedance and admittance [17]. Finally, a state space representation and an equivalent SPICE circuit can be synthesized for the $\boldsymbol{Z}$ matrix, by using standard realization [24] and circuit synthesis techniques [25].

A. Additional weighting function

An additional least-squares weighting function can be added to the parametric macromodeling algorithm, when the elements to fit have a high dynamic range. It improves the relative accuracy where the elements to fit are small in their dynamic range [29] and is chosen equal to the inverse of the element magnitude:

$$w_{H_i}(s,g)_k = |(H_i(s,g)_k)^{-1}| \tag{10}$$

for $i = 1, ..., M$, where M is the maximum number of functions fitted with common poles in the same least-squares matrix. The RMS-error is chosen to characterize the model accuracy. It is weighted if the previous weighting function is used during the modeling process.

$$RMS = \sqrt{\frac{1}{MK}\sum_{i=1}^{M}\sum_{k=1}^{K}\left|R_i(s,g)_k - H_i(s,g)_k\right|^2} \tag{11}$$

$$RMS_{weighted} = \\ = \sqrt{\frac{1}{MK}\sum_{i=1}^{M}\sum_{k=1}^{K}\left|w_{H_i}(s,g)_k\Big(R_i(s,g)_k - H_i(s,g)_k\Big)\right|^2} \tag{12}$$

B. Mode selection

The infinite sum in (5) must be truncated in order to obtain a finite rational representation of the multiconductor transmission line. A bottom-up strategy based on the check of the dominant poles of the modal impedances $\boldsymbol{Z}_n$ is followed to select the number of modes. The check of the dominant poles used in this work extends the algorithm presented in [30] by looking at the ratio between the residues and the real part of the corresponding poles in the second step of the procedure. $\boldsymbol{Z}_n$ are evaluated on the minimum, mean and maximum values of each design parameter range. If for a certain number mode n all checks prove that the dominant poles are out of a defined bandwidth $\xi\omega_{max}$ (where $\xi > 1$), the algorithm ends and the number of modes is equal to $n-1$. The algorithm is described for the bivariate case, but the full multivariate formulation is similar.

Input: Parametric macromodels $\tilde{\boldsymbol{Z}}_{pul}(s,g)$, $\tilde{\boldsymbol{Y}}_{pul}(s,g)$
Output: Number of modes n_{modes}

Multivariate to Univariate [23]: $\tilde{\boldsymbol{Z}}_{pul}(s,g)$, $\tilde{\boldsymbol{Y}}_{pul}(s,g) \longrightarrow$ $\tilde{\boldsymbol{Z}}_{pul}(s,g_i)$, $\tilde{\boldsymbol{Y}}_{pul}(s,g_i)$, g_i=$\{g_{min}, g_{mean}, g_{max}\}$.

$convergence = false$;
$\xi > 1, \;\; 0 < \zeta < 1$;
$n = 0$;

while $convergence = false$ **do**
  %Pole check
  foreach g_i **do**
    $[poles_n, residues_n] = poles\_residues\_mode(\tilde{\boldsymbol{Z}}_{pul}(s,g_i), \tilde{\boldsymbol{Y}}_{pul}(s,g_i), n)$ ([17]);
    foreach $pole_n$ **do**
      foreach $residue_n$ **do**
        if $|Im(pole_n)| < \xi\omega_{max} \cap |residue_n/Re(pole_n)| > \zeta max(|residues_n/Re(poles_n)|)$ **then**
          $n = n + 1$;
          go to foreach g_i **do**
        end
      end
    end
  end
  $convergence = true$
end

$n_{modes} = n - 1$.

Algorithm 1: *Mode selection.*

IV. Numerical results

Two coupled microstrips with frequency-dependent per-unit-length parameters and linear terminations

A three-conductor transmission line (length $\ell = 15$ cm) with frequency-dependent per-unit-length parameters has been modeled. It consists of two coplanar microstrips over a ground plane. The cross sections is shown in Fig. 1. The conductors have width $w = 100$ μm and thickness $t = 50$ μm. The spacing S between the microstrips is considered as design parameter in addition to frequency. The dielectric is 300 μm thick and characterized by a dispersive and lossy permittivity which has been modeled by the wideband Debye model [31]. The infinite series in (5) has been truncated to $n_{modes} = 34$. The ranges of frequency and spacing are $freq \in [1 \cdot 10^5 - 15 \cdot 10^9]$ Hz and $S \in [100 - 500]$ μm.

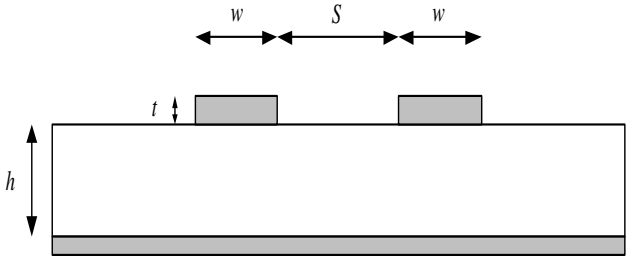

Fig. 1. Cross section of the two coupled microstrips.

The frequency-dependent per-unit-length parameters have been evaluated using a commercial tool [32] over a reference grid of 250×40 samples, for frequency and spacing respectively. We have utilized 30×10 samples of the previous grid and set the number of poles equal to 4 and 2 for frequency and spacing, to model the per-unit-length admittance and impedance functions. The RMS and $RMS_{weighted}$ errors of

the corresponding parametric macromodels over the reference grid are equal to $1 \cdot 10^{-5}$ and $3 \cdot 10^{-5}$. The magnitude of the parametric macromodels of $Z_{pul,(12)}$ is shown in Fig. 2.

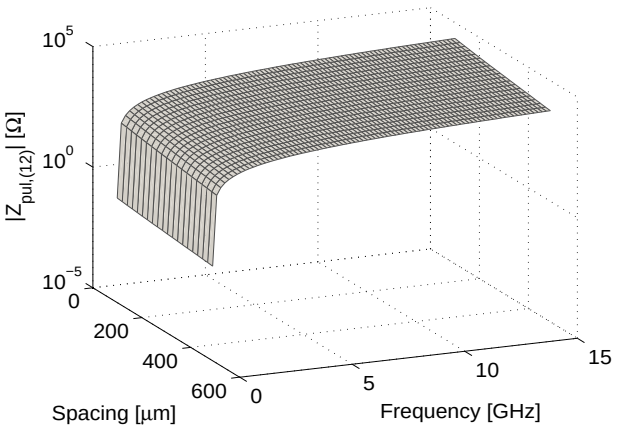

Fig. 2. Magnitude of the parametric macromodel of $Z_{pul,(12)}$.

Subsequently, these parametric macromodels have been reduced to univariate frequency-dependent functions for the set of spacing values $S = \{131, 233, 346, 449\}$ μm. These points have not been used for the generation of the macromodels. Then, the univariate macromodels of the modal impedances have been computed for the previous set of spacing points. The magnitude and phase of $Z_{n,(12)}$ computed from the per-unit-length impedance and admittance data and its respective macromodels are shown in Figs. 3-4 for modes $n = \{0, 1, 13\}$, $S = 346$ μm, for validation purpose. A good satisfactory agreement is obtained between the original raw data and the macromodels.

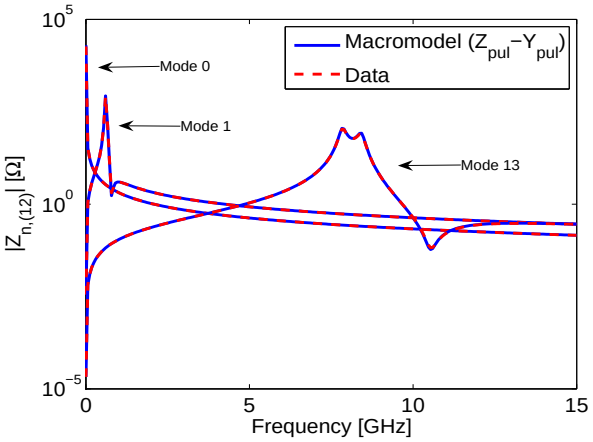

Fig. 3. Magnitude of $Z_{n,(12)}$ (modes $n = \{0, 1, 13\}$, $S = 346$ μm).

The macromodel of the $\boldsymbol{Z}$ matrix, composed of the sum of 34 modes, for a certain fixed spacing, can be built by using the corresponding macromodels of the modal impedances. The

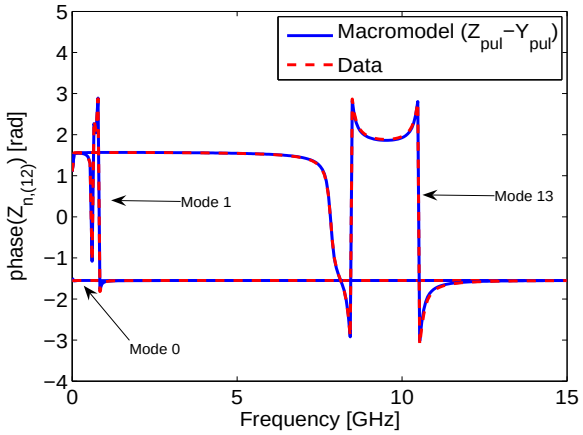

Fig. 4. Phase of $Z_{n,(12)}$ (modes $n = \{0, 1, 13\}$, $S = 346$ μm).

$RMS_{weighted}$ error between the univariate macromodels of the $\boldsymbol{Z}$ matrix and its computation from the exact transmission line theory (TLT) over the reference grid is equal to $5 \cdot 10^{-4}$. The magnitude of Z_{14} computed by TLT over the reference grid is shown in Fig. 5. The magnitude and the phase of the macromodel of Z_{14} are compared with the results obtained from TLT in Figs. 6-7 for $S = 131$ μm.

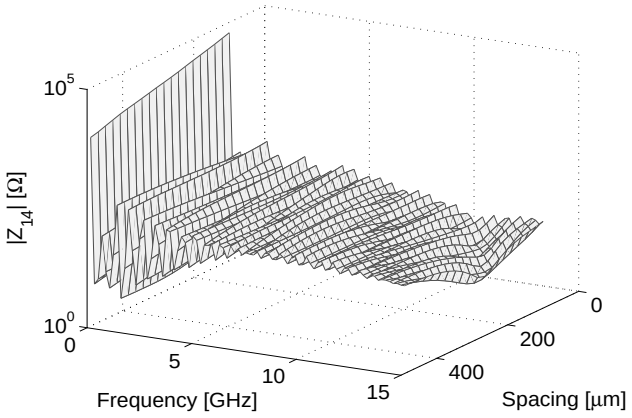

Fig. 5. Magnitude of Z_{14} (TLT).

The results show the high accuracy of the parametric macromodeling strategy in frequency domain. The next step is to show that the accuracy is preserved in time-domain as well. One line has been excited by an impulsive voltage source with amplitude 1 V, rise/fall times $\tau_r = \tau_f = 400$ ps and width 1.5 ns. The victim line have been terminated on the near and far-end by $R_{NE} = 50$ Ω and $R_{FE} = 50$ Ω, $C_{FE} = 1$ pF, while the driven line has been terminated on a driver and load impedance equal to $R_S = 50$ Ω and $R_L = 50$ Ω, $C_L = 1$ pF (see Fig. 8). The port voltages have been computed using the exact transmission line theory (TLT-IFFT) and a state-space

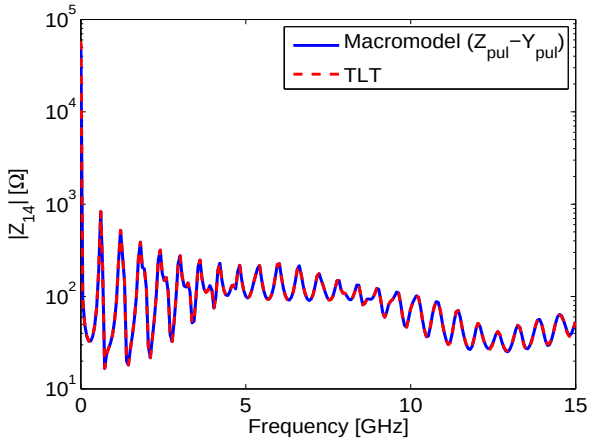

Fig. 6. Magnitude of Z_{14} ($S = 131$ μm).

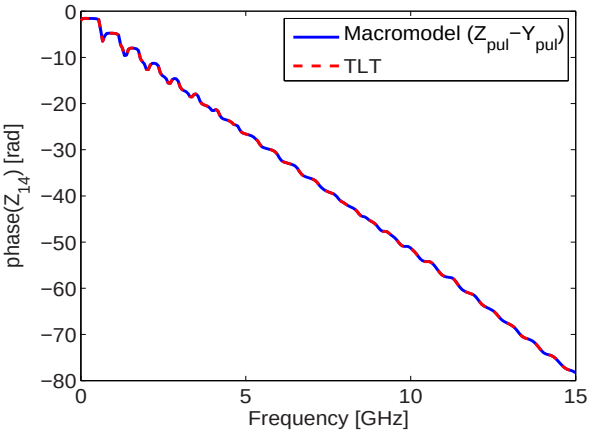

Fig. 7. Phase of Z_{14} ($S = 131$ μm).

realization of the frequency domain macromodel of the $\boldsymbol{Z}$ matrix. Time domain results are shown in Figs. 9-10 for the set of spacing values $S = \{131, 233, 346, 449\}$ μm.

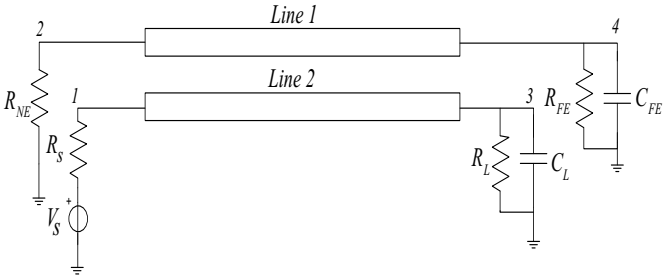

Fig. 8. Two coupled microstrips with linear terminations.

The port voltages results in time-domain confirm that the parametric macromodeling algorithm captures and describes second order phenomena, as the crosstalk, accurately.

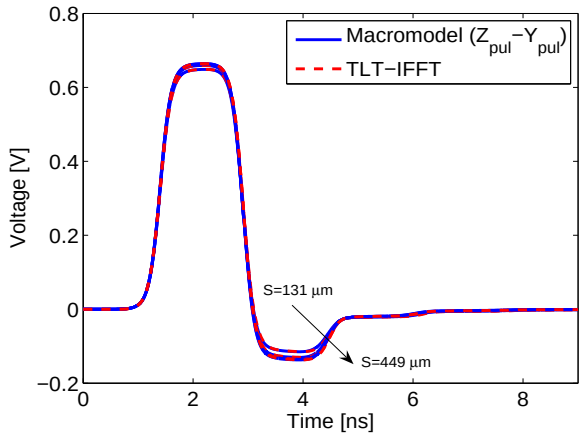

Fig. 9. Input voltage of the driven line terminated on $R_S = 50$ Ω and $R_L = 50$ Ω, $C_L = 1$ pF ($S = \{131, 233, 346, 449\}$ μm).

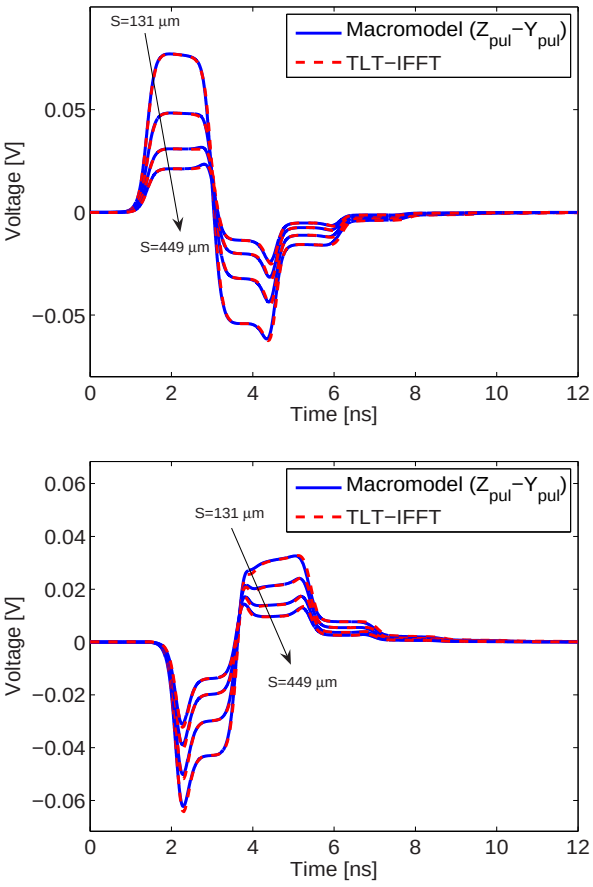

Fig. 10. Input and output voltages of the victim line terminated on $R_{NE} = 50$ Ω and $R_{FE} = 50$ Ω, $C_{FE} = 1$ pF ($S = \{131, 233, 346, 449\}$ μm).

V. Conclusions

Many second order effects, such as delay, coupling and crosstalk, have become prominent because of increased in-

tegration levels and signal speeds. Accurate prediction of these interconnects effects is fundamental for a successful design and often prohibitively CPU expensive. Design space exploration, design optimization and crosstalk analysis are involved in the design framework in addition to regular simulations. The crosstalk between closely spaced signal lines limits interconnect performance and becomes an important design aspect. Parametric macromodeling techniques are needed to make efficient these design activities. We have presented an innovative parametric macromodeling approach for lossy and dispersive multiconductor transmission lines. It has been found capable to generate accurate rational macromodels with respect to physical and geometrical parameters. The spectral decomposition of the impedance matrix $\boldsymbol{Z}$ is exploited to simplify the system identification process significantly. The numerical results have validated the proposed technique and confirmed its accuracy and effectiveness in capturing second order phenomena, as the crosstalk, which are crucial in the analysis and design of high-speed interconnects.

REFERENCES

[1] A. Deutsch, "Electrical characteristics of interconnects for high-performance systems," *Proc. IEEE, invited paper*, vol. 86, no. 2, pp. 315–355, 1998.

[2] M. Nakhla and R. Achar, *Handbook on VLSI*. Boca Raton, FL: CRC, 2000.

[3] C. R. Paul, *Analysis of Multiconductor Transmission Lines*, 2nd ed. New York, NY: John Wiley & Sons, 2008.

[4] R. Achar, M. Nakhla, "Simulation of high-speed interconnects," *Proceedings of the IEEE*, vol. 89, no. 5, pp. 693–728, May 2001.

[5] F. Y. Chang, "The generalized method of characteristics for waveform relaxation analysis of lossy coupled transmission lines," *IEEE Transactions on Microwave Theory and Techniques*, vol. 37, no. 12, pp. 2028–2038, Dec. 1989.

[6] A. Odabasioglu, M. Celik, and L. T. Pileggi, "PRIMA: passive reduced-order interconnect macromodeling algorithm," *IEEE Transactions on Computer-Aided Design*, vol. 17, no. 8, pp. 645–654, Aug. 1998.

[7] Q. Yu, J. M. L. Wang and E. S. Kuh, "Passive multipoint moment matching model order reduction algorithm on multiport distributed interconnect networks," *IEEE Transactions on Circuits and Systems, I*, vol. 46, no. 1, pp. 140–160, Jan. 1999.

[8] A. C. Cangellaris, S. Pasha, J. Prince and M. Celik, "A new discrete time-domain model for passive model order reduction and macromodeling of high-speed interconnections," *IEEE Transactions on Comp. Packag. Technol.*, vol. 22, pp. 356–364, Aug. 1999.

[9] A. Dounavis, X. Li, M. S. Nakhla, R. Achar, "Passive closed-form transmission-line model for general-purpose circuit simulators," *IEEE Transactions on Microwave Theory and Techniques*, vol. 47, no. 12, pp. 2450–2459, Dec. 1999.

[10] A. Dounavis, E. Gad, R. Achar, M. S. Nakhla, "Passive model reduction of multiport distributed interconnects," *IEEE Transactions on Microwave Theory and Techniques*, vol. 48, no. 12, pp. 2325–2334, Dec. 2000.

[11] R. Achar, P.K. Gunupudi, M. Nakhla, E. Chiprout, "Passive interconnect reduction algorithm for distributed/measured networks," *IEEE Transactions on Circuits and Systems, II*, vol. 47, no. 4, pp. 287–301, Apr. 2000.

[12] A. Dounavis, R. Achar and M. Nakhla, "Addressing transient errors in passive macromodels of distributed transmission-line networks," *IEEE Transactions on Microwave Theory and Techniques*, vol. 50, no. 12, pp. 2759–1768, Dec. 2002.

[13] L. F. Knockaert, D. De Zutter, F. Olyslager, E. Laermans, and J. De Geest, "Recovering lossy multiconductor transmission line parameters from impedance or scattering representations," *IEEE Transactions on Advanced Packaging*, vol. 25, no. 2, pp. 200–205, May 2002.

[14] E. Gad and M. Nakhla, "Efficient simulation of nonuniform transmission lines using integrated congruence transform," *IEEE Transactions on Very Large Scale Integration (VLSI) Systems*, vol. 12, no. 12, pp. 1307–1320, Dec. 2004.

[15] N. M. Nakhla, A. Dounavis, R. Achar and M. S. Nakhla, "DEPACT: delay extraction-based passive compact transmission-line macromodeling algorithm," *IEEE Transactions on Advanced Packaging*, vol. 28, no. 1, pp. 13–23, Feb. 2005.

[16] C. Chen, E. Gad, M. Nakhla and R. Achar, "Analysis of frequency-dependent interconnects using integrated congruence transform," *IEEE Transactions on Computer-Aided Design*, vol. 26, no. 6, pp. 1139–1149, June 2007.

[17] G. Antonini, "A dyadic Green's function based method for the transient analysis of lossy and dispersive multiconductor transmission lines," *IEEE Transactions on Microwave Theory and Techniques*, vol. 56, no. 4, pp. 880–895, Apr. 2008.

[18] L. B. Gravelle and P. F. Wilson, "EMI/EMC in printed circuit boards - a literature review," *IEEE Transactions on Electromagnetic Compatibility*, vol. 34, no. 2, pp. 109–116, May 1992.

[19] M. Goldfarb and A. Platzker, "The effects of electromagnetic coupling on MMIC design," *Int. J. Microwave Millimeter Wave CAE*, vol. 1, no. 1, pp. 38–47, 1991.

[20] P. Gunupudi, R. Khazaka, and M. Nakhla, "Analysis of transmission line circuits using multidimensional model reduction techniques," *IEEE Transactions on Advanced Packaging*, vol. 25, no. 2, pp. 174–180, May 2002.

[21] P. K. Gunupudi, R. Khazaka, M. S. Nakhla, T. Smy, and D. Celo, "Passive parameterized time-domain macromodels for high-speed transmission-line networks," *IEEE Transactions on Microwave Theory and Techniques*, vol. 51, no. 12, pp. 2347–2354, Dec. 2003.

[22] S. Grivet-Talocia, S. Acquadro, M. Bandinu, F. G. Canavero, I. Kelander, M. Rouvala, "A parameterization scheme for lossy transmission line macromodels with application to high speed interconnects in mobile devices," *IEEE Transactions on Electromagnetic Compatibility*, vol. 49, no. 1, pp. 18–24, Feb. 2007.

[23] D. Deschrijver, T. Dhaene and D. De Zutter, "Robust parametric macromodeling using multivariate orthonormal vector fitting," *IEEE Transactions on Microwave Theory and Techniques*, vol. 56, no. 7, pp. 1661–1667, July 2008.

[24] R. Achar, M. Nakhla, "Simulation of high-speed interconnects," *Proceedings of the IEEE*, vol. 89, no. 5, pp. 693–728, May 2001.

[25] G. Antonini, "Spice equivalent circuits of frequency-domain responses," *IEEE Transactions on Electromagnetic Compatibility*, vol. 45, no. 3, pp. 502–512, Aug. 2003.

[26] A. R. Djordjevic, M. B. Bazdar, T. K. Sarkar, R. F. Harrington, *Matrix parameters for multiconductor transmission lines*. Boston London: Artech House Publishers, 2000.

[27] B. Gustavsen, "Enforcing passivity for admittance matrices approximated by rational functions," *IEEE Transactions on Power Delivery*, vol. 16, no. 1, pp. 97–104, Feb. 2001.

[28] D. Saraswat, R. Achar and M. S. Nakhla, "Global passivity enforcement algorithm for macromodels of interconnect subnetworks characterized by tabultaed data," *IEEE Transactions on Very Large Scale Integration (VLSI) Systems*, vol. 13, no. 7, pp. 819 – 832, July 2005.

[29] B. Gustavsen, "Relaxed vector fitting algorithm for rational approximation of frequency domain responses," *Proc. in Workshop Signal Propagation on Interconnects*, vol. 21, no. 3, pp. 1587–1592, May 2006.

[30] G. Antonini, "A new methodology for the transient analysis of lossy and dispersive multiconductor transmission lines," *IEEE Transactions on Microwave Theory and Techniques*, vol. 52, no. 9, pp. 2227–2239, Sept. 2004.

[31] A.R.Djordjević, R.M. Biljić, V.D. Likar-Smiljanić, T.K. Sarkar, "Wideband frequency-domain characterization of FR-4 and time-domain causality," *IEEE Transactions on Electromagnetic Compatibility*, vol. 43, no. 4, pp. 662–667, Nov. 2001.

[32] *Simbeor, Electromagnetic Simulation Environment with 3D Full-Wave Field Solver for Multi-Layered Circuits*, Simberian Inc., Seattle.